

MODELING THE EQUILIBRIUM COMPRESSED VOID VOLUME OF CARBON BLACK

GEORGE A JOYCE, * WILLIAM M HENRY

COLUMBIAN CHEMICALS COMPANY
MARIETTA, GA

ABSTRACT

In this study, a broad range of furnace carbon blacks from very low to very high structure and fineness were evaluated for compressed void volume, colloidal and in-rubber properties. Compressed void volume measurements were investigated over applied pressures of approximately 18-159 MPa using a commercially available instrument. The void volume data was statistically modeled using logarithmic pressure curves, exponential energy curves and an inverse variable root curve. Parameters generated from the void volume models were analyzed using advanced non-linear multiple regression resulting in strong relationships to crushed oil absorption numbers and in-rubber properties. A comparison of void volume and oil absorption numbers indicates the void volume method offers a significant improvement in describing carbon black structure. The relationship between void volume and parameters related to rubber reinforcement found in this work is a confirmation that compressed void volume is more specific to primary structure than oil absorption numbers. Compressed void volume should provide the carbon black industry a faster, more meaningful and lower cost structure characterization than oil absorption methods.

INTRODUCTION

Today, the carbon black industry uses a set of colloidal quality tests that have been in use for more than forty years. The most important of these quality tests are surface area and structure measurements. Surface area is typically estimated using iodine adsorption number, while nitrogen surface area (NSA) and statistical thickness surface area (STSA) are specific surface area measures. Carbon black structure is measured by oil absorption methods including oil absorption number (OAN), and oil absorption number of compressed sample (COAN). Surface area and structure tests along with other predictor tests are used to define most carbon black production. The fundamental properties of carbon black including particle size distribution, aggregate size and shape distributions, porosity and surface chemistry are too complex to be easily or quickly characterized in a production laboratory.

The term "carbon black structure" is defined by ASTM International Standard D3053 as "the quality of irregularity and deviation from sphericity of the shape of a carbon black aggregate". Primary structure is a term used to describe the irregularity and deviation from sphericity of individual aggregates in a carbon black sample. However this bulk description is at best an average of the geometrical distribution of shapes and sizes of the aggregates in the carbon black sample. Secondary or transient structure is a term used to describe an agglomeration of aggregates, held together by Van der Waals forces that are formed within the process. The primary structure undergoes only minor breakdown during mixing and dispersion, and requires a large energy to fracture. Secondary structure is readily disrupted during processing and can be reversible.

In a rubber compound the carbon black surface area, surface activity and structure are the most important properties affecting processability and reinforcement through mechanisms including polymer immobilization and polymer occlusion. Polymer immobilization is mostly dependent on carbon black surface properties and is similar for many furnace rubber blacks. Polymer occlusion is dependent on the carbon black structure, with the primary structure being responsible for many of the ultimate mechanical properties of well dispersed carbon black-rubber compounds.

* Corresponding author. Ph: 770-792-9467; Fax: 770-792-9631; email: gjoyce@columbianchemicals.com

The carbon black industry utilizes OAN as a measure of the structure of carbon black to the point of being a critical parameter in the specification of a carbon black grade. Unfortunately, OAN is a very limited measure and often does not correlate well with compound performance that depends on carbon black structure. This has led the industry to incorporate additional tests such as COAN that minimize effects of secondary structure in the oil absorption test, which provides a better relationship to in-rubber properties. Another more direct measurement utilized by the industry is transmission electron microscopy (TEM) that is useful for analyzing the size and shape distribution of carbon black aggregates, but is very costly and provides no information related to secondary structure. The industry needs a single experimental technique that can provide information on both the primary and secondary structure in a carbon black sample. Void volume provides a tool with the potential to meet the needs for an improved methodology to measure carbon black structure. Unfortunately, this methodology has required significant improvements in instrumentation and microprocessor based equipment that up until recently prevented its development as a mature and reliable technique that could be applied industry-wide.

In this study we investigate new advances in the experimental measurement of the volume changes in a carbon black as a function of pressure (compression force). This change in volume, defined as void volume, has been related to the structure in a carbon black sample. The results are correlated to OAN, COAN and in-rubber properties and are discussed as an improved methodology that can replace OAN as a standard technique for the measurement of structure in the carbon black industry.

EXPERIMENTAL

CARBON BLACKS

A broad range of commercial and experimental furnace carbon blacks from very low ($\sim 35 \text{ cm}^3/100\text{g}$) to very high ($\sim 175 \text{ cm}^3/100\text{g}$) OAN were selected for study. The carbon blacks include a variety of Statex[®], Furnex[®] and experimental furnace carbon blacks from Columbian Chemicals Company along with Standard Reference Blacks (SRB) from ASTM International including the SRB Series 5 and 6 materials and two experimental OAN standards. One sample of N990 thermal black was included in the SRB series (G-6). Partially graphitized carbon blacks including Pureblack[®] from Columbian Chemicals Company-Superior Graphite were also included in this study. Several powder blacks were obtained along with corresponding pelleted products. The colloidal space covered by these carbon black samples is shown in Figure 1.

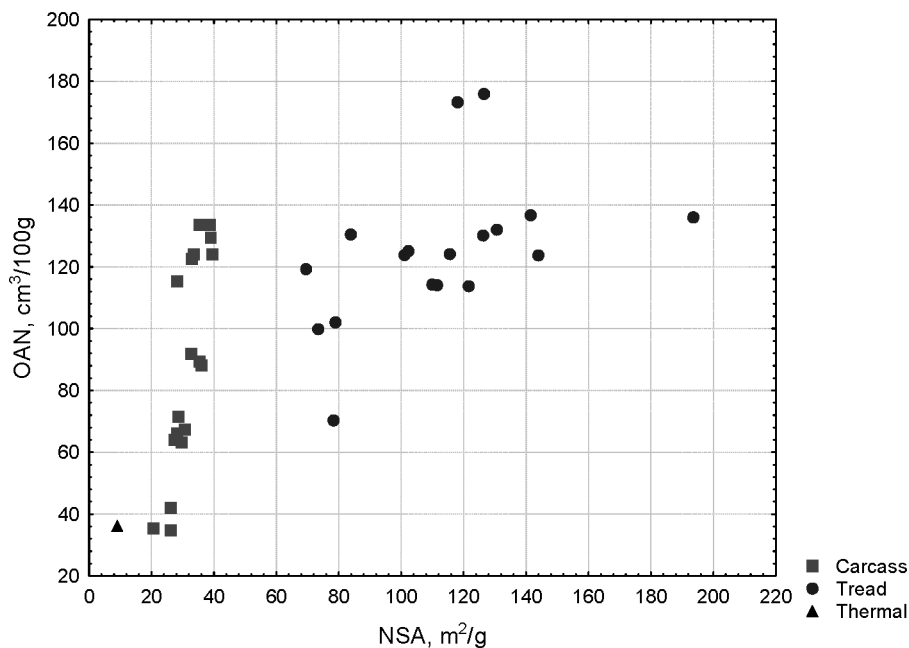


FIG. 1. — Sample colloidal space.

VOID VOLUME INSTRUMENT

Multi-point equilibrium compressed void volume data was obtained on all samples using an instrument from Jaron Technologies per ASTM International D6086-05. Compressed void volume data was obtained at an ambient temperature of 23 ± 2 °C over applied pressures of approximately 18-159 MPa (constant stress). The sample cylinder is 1.27 cm (0.500 inch) in diameter and has a piston travel of approximately 13.6 cm (5.35 inches). The cylinder surfaces were finished using a proprietary process. The piston is driven using a pneumatic control cylinder with a diameter of 20.32 cm (8 inch) and does not incorporate stress rate control. Pressure is controlled using a precision regulator and is measured using a digital transducer. Instrument control is based on a modern programmable logic controller (PLC) and interface. A schematic of key components of a void volume instrument is shown in Figure 2.

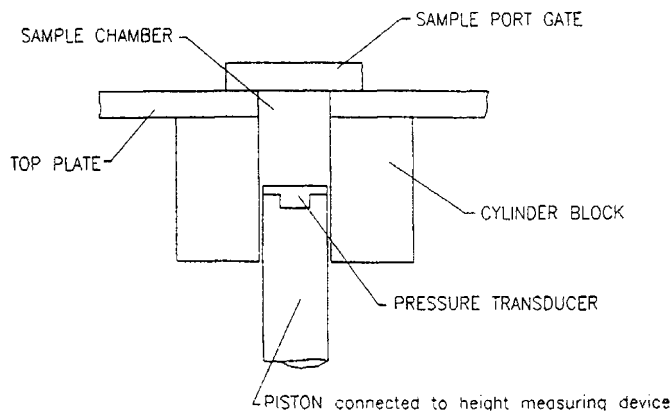


FIG. 2. — Reprinted, with permission, from D6086-05 Standard Test Methods for Carbon Black—Compressed Volume Index, copyright ASTM International, 100 Barr Harbor Drive, West Conshohocken, PA 19428.

Of particular importance are the height and pressure measuring devices, and the cylinder wall finish. The Jaron instrument measures pressure applied to the piston via the pneumatic control cylinder, and is pre-programmed for a 2.0 g sample mass and 60 s compression period. Calibration of height measurement is achieved using steel calibration plugs.

The calculation of compressed void volume (VV) is shown in Equation 1:¹

$$VV = V_A - V_T \quad (1)$$

where V_A is equal to the actual compressed volume of the sample in cm^3 , and V_T is equal to the theoretical volume of the sample in cm^3 . The actual compressed volume, V_A , is defined by Equation 2:

$$V_A = \frac{h \times \pi D^2}{4} \quad (2)$$

where h equals the measured sample height in cm, and D is equal to the cylinder diameter in cm. The theoretical sample volume, V_T , is defined by Equation 3:

$$V_T = \frac{m}{d} \quad (3)$$

where m is the sample mass in grams and d is the accepted density of carbon black equal to 1.9 g per cm^3 .²

OTHER TESTING

The rubber carbon blacks were also analyzed for colloidal properties including nitrogen surface area per ASTM International D6556, OAN per ASTM International D2414, and COAN per ASTM International D3493. Pour density was obtained on the pelleted blacks per ASTM International D1513. Most of the colloidal properties for the SRB blacks were obtained from ASTM International D4821 or ASTM International laboratory proficiency rating system (LPRS) studies.

In-rubber rheometer and dynamic properties were obtained using an Alpha Technologies RPA 2000 per ASTM International D6601. Test compounds included styrene-butadiene rubber (SBR) and natural rubber (NR) formulations per ASTM International D3191 and D3192, respectively. The rheometer properties were obtained at 150 °C using 30 minute cures and dynamic properties at 100 °C at 1 Hz and 1, 10 and 50 percent single strain amplitude (SSA).

MODELING

Modeling of the equilibrium compressed void volume data in this study focuses primarily on the fitting of experimental data to various sets of equations in an effort to more accurately describe the fundamental void space characteristics of carbon black structure at different levels of applied pressure, and to establish mathematical relationships that exist between void volume, colloidal, and in-rubber properties.

To begin with, an examination was made of the void volume pressure curves for each carbon black tested. This method consisted of statistically analyzing void volume data over nine

equal intervals of applied pressure from 18 MPa to 159 MPa. There were two advanced linear and nonlinear models used for this analysis.³ From these results, various advanced regression models were analyzed for predicting colloidal and in-rubber properties using interactive, polynomial, and interactive by polynomial effects for multiple void volume measurement parameters at different levels of applied pressure. After establishing the best fit predictive models for each sample of carbon black, a data table was generated containing calculated void volume results for each unit of pressure (MPa) over the entire pressure range (fitted data). Where applicable, these prediction models for colloidal and compound properties were then applied to each unit of pressure for all carbon black samples in the data table, and coefficients of determination (R^2) were generated for each model for each unit of applied pressure. The primary objective of this analysis was to identify the different levels of applied pressure necessary to produce the best relationships between void volume and several carbon black dependent properties.

A general linear model was used to determine the relationship between the logarithm of applied pressure and the resulting void volume of carbon black. Previous studies by Medalia⁴ identified this type model as a good fit for the thickness of compressed carbon black samples under different levels of applied pressure. It can be verified that the compressed void volume instrument calculations used in this investigation are linear to the height (or thickness) of the compressed carbon black sample as shown in Figure 3. For this equipment, at an uncompressed piston height of approximately 13.6 cm, void volume is equal to 846.4 cm³/100g. As a result, the uncompressed cylinder volume is sufficiently large for very low density (powder) carbon blacks.

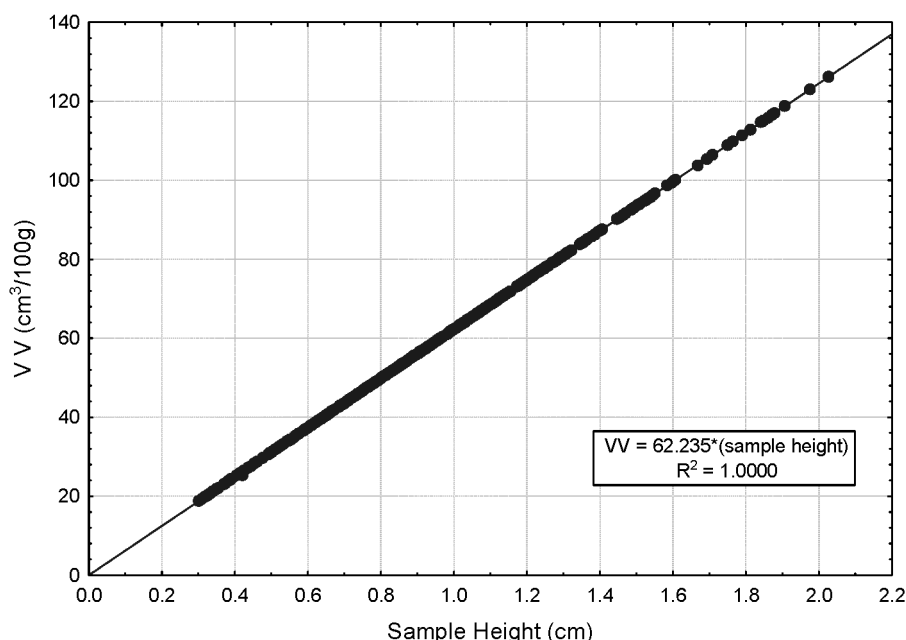


FIG. 3. — Void volume - Sample height relationship.

The second type of advanced modeling technique used to fit applied pressure and void volume data was a nonlinear estimate based on specified regression functions. Several sets of nonlinear equations were investigated in order to obtain additional dry bulk compression parameters for accurately characterizing carbon black structure. This method of modeling involves selecting a family of curves with starting parametric values that closely resemble the graphical representation of observed data, and then iterating these values until a convergence criterion can be met

based on minimizing least square regression errors. One of the curve families used in this investigation contains three parameters a , b , and c :

$$Y = \frac{1}{(a + b \times X^c)} \quad (4)$$

By selecting three points along the curve (X_1, Y_1) , (X_2, Y_2) , and (X_3, Y_3) such that $X_1^2 = X_2 * X_3$, the following Equations 5-7 can be used to calculate the curve parameters⁵ thereby minimizing the required number of experimental measurements:

$$a = \frac{(Y_2 Y_3 - Y_1^2)}{(2(Y_1 Y_2 Y_3) - Y_1^2(Y_2 + Y_3))} \quad (5)$$

$$b = \frac{(1 - aY)}{(Y_1 X_1^c)} \quad (6)$$

$$c = \frac{\ln\left(\frac{(Y_2 - aY_1 Y_2)}{(Y_1 - aY_1 Y_2)}\right)}{\ln\left(\frac{X_1}{X_2}\right)} \quad (7)$$

RESULTS

PRECISION ESTIMATE FOR COMPRESSED VOID VOLUME

The repeatability estimate (R_c) of the void volume measurements was analyzed over the entire pressure range under study in order to understand the error contribution in models based on VV testing. An ASTM International SRB carbon black (B5) was tested a total of twenty times over nine applied pressures on a daily basis. The repeatability of the VV analysis for the equipment used in this study varied from 1.85 cm³/100g at high pressure to 4.14 cm³/100g at low pressure with a pooled value of 2.87 cm³/100g. The following table contains statistics for each pressure interval.

TABLE I
COMPRESSED VOID VOLUME REPEATABILITY PARAMETERS

Applied Pressure (MPa)	Mean	n	Standard Deviation	Re
17.7	81.66	20	1.46	4.14
35.3	70.13	20	1.04	2.93
53.0	63.65	20	1.09	3.09
70.6	58.81	20	0.79	2.24
88.3	55.15	20	0.77	2.18
105.9	52.35	20	0.93	2.63
123.6	49.59	20	1.13	3.19
141.2	47.01	20	0.79	2.24
158.9	45.02	20	0.65	1.85
Pooled			1.01	2.87

Since void volume is a function of applied pressure, a significant contribution to the VV repeatability error is believed to be related to positioning of the manually controlled pressure regulator. Small differences in applied pressure to the control cylinder have a large effect on pressure applied to the sample. Every 6.89×10^{-3} MPa (1 psi) change in control pressure is equivalent to 1.72 MPa (250 psi) pressure applied to the sample. An improvement in control pressure such as a digitally controlled regulator should result in reduced VV error. In addition to the regulator, the pressure measurement system must be very accurate and repeatable in order to minimize error. Finally, normalization of test results to SRB target values would further improve VV testing precision.

By comparison, OAN precision is reported after normalization with SRB standards since the absolute measurement is too variable between instruments and mixing chambers. The OAN pooled repeatability per ASTM International D2414 is $1.8 \text{ cm}^3/100\text{g}$ for a two-day precision estimate. This OAN repeatability estimate would increase without normalization or if measured over a longer time period. A better comparison of long-term OAN repeatability was obtained using ASTM International SRB F-6 carbon black. Twenty daily measurements of F-6 were selected from a single absorptometer-mixing chamber assembly using non-normalized data. The repeatability estimate is seen in Table II.

TABLE II
OAN REPEATABILITY PARAMETERS

Mean	n	Standard Deviation	Re
132.6	20	1.24	3.52

Based on this analysis and previous studies⁶ of long-term and non-normalized precision, the observed repeatability of compressed void volume appears to be effectively superior to OAN. Further analyses of short and long-term precision are needed along with the use of standard reference blacks to better understand the precision of VV across all carbon black grades.

MODELING COMPRESSION CHARACTERISTICS OF CARBON BLACK

Log Pressure Model. — Earlier modeling of void volume as a function of pressure indicated a linear relationship exists between VV and the logarithm of pressure.^{4,7} Examples of VV ver-

sus pressure curves are shown in Figure 4. It is clear from this figure that void volume does not behave linearly with applied pressure. Non-linearity seemingly increases with increasing structure level as analyzed by OAN. In Figure 5, VV is plotted against the logarithm of applied pressure ($\log_{10} P$). In this case a high degree of linearity is observed for all curves and the regression coefficients can be calculated for the model equation:

$$VV = A_1 + B_1 \log_{10} P \tag{8}$$

Table III provides the calculated regression coefficients A_1 and B_1 for all carbon blacks in this work. The predicted VV is plotted against the experimental values in Figure 6.

TABLE III
 LOG PRESSURE MODEL PARAMETERS AND COEFFICIENTS OF DETERMINATION

Sample	Grade	A ₁	B ₁	R ²	Sample	Grade	A ₁	B ₁	R ²
1	N762	83.122	-23.363	0.9981	28	N650H 1000	132.437	-41.230	0.9996
2	N660	102.159	-28.637	0.9968	29	N650H 1100	127.760	-40.817	0.9994
3	N650	130.114	-39.222	0.9980	30	N650H 1500	114.996	-39.189	0.9997
4	N220	141.557	-39.709	0.9979	31	N774	82.691	-20.789	0.9944
5	HV3396	184.283	-56.379	0.9984	32	N774P	92.556	-24.452	0.9923
6	N650	128.461	-38.320	0.9992	33	N339P	184.307	-58.810	0.9805
7	N299	151.913	-44.187	0.9994	34	N550P	140.729	-44.203	0.9911
8	N234	157.688	-45.635	0.9988	35	N339	146.792	-41.447	0.9956
9	N347	159.379	-47.977	0.9995	36	N550	128.999	-38.511	0.9970
10	N550	132.735	-40.177	0.9983	37	HV3396P	193.709	-61.244	0.9679
11	N299	148.708	-42.764	0.9990	38	HV3396	176.505	-52.240	0.9992
12	N330	129.925	-36.640	0.9991	39	N135	172.381	-50.933	0.9995
13	N762	77.367	-20.066	0.9974	40	N134	188.266	-58.984	0.9978
14	N774	84.142	-22.561	0.9980	41	N330	129.602	-38.095	0.9996
15	N121	174.612	-52.086	0.9996	42	N220	161.375	-49.056	0.9992
16	N121 HT1500	198.893	-69.565	0.9904	43	N220	159.206	-48.178	0.9998
17	N121	185.364	-57.009	0.9972	44	N326	96.537	-25.728	0.9978
18	N121 HT1000	193.414	-62.230	0.9977	45	N762	76.374	-20.926	0.9965
19	CD1006	49.252	-13.617	0.9942	46	N762	86.391	-24.380	0.9990
20	CD1003	52.706	-12.826	0.9932	47	N660	111.987	-33.561	0.9935
21	CD1001	123.648	-36.298	0.9989	48	N660	105.329	-29.219	0.9973
22	CD2005 HT1000	190.994	-62.390	0.9846	49	N683	148.629	-45.485	0.9996
23	CD2005 HT1500	184.948	-65.791	0.9948	50	N683	149.663	-45.920	0.9997
24	CD2005 HT2000	182.121	-63.687	0.9900	51	N990	48.029	-12.444	0.9922
25	CD2005	187.320	-55.980	0.9975	52	N100	211.774	-68.478	0.9970
26	PB-115	147.349	-48.577	0.9979	53	N700	46.929	-12.377	0.9929
27	N650H	135.421	-41.065	0.9992	54	N351	149.842	-44.558	0.9999

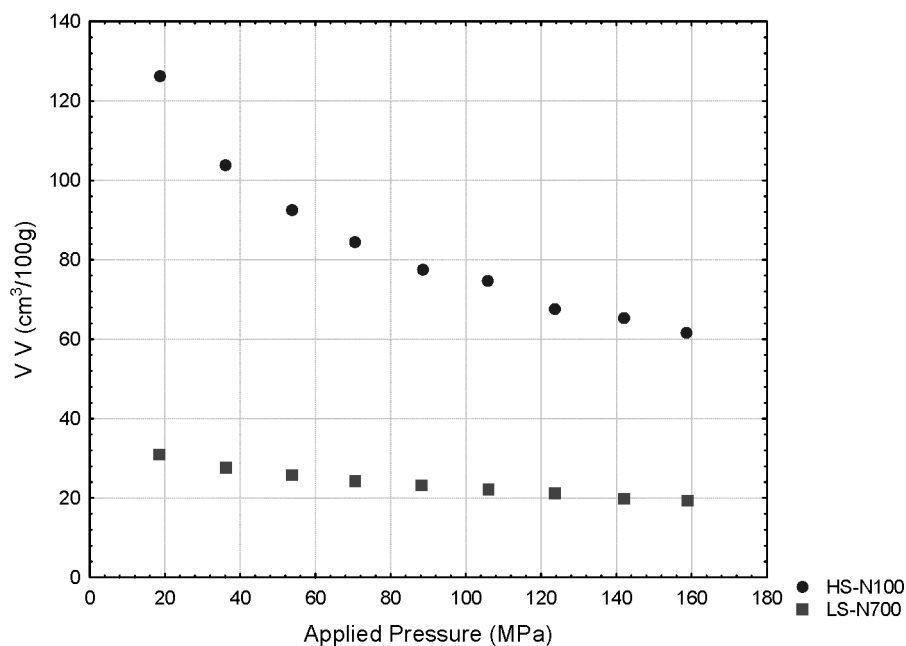
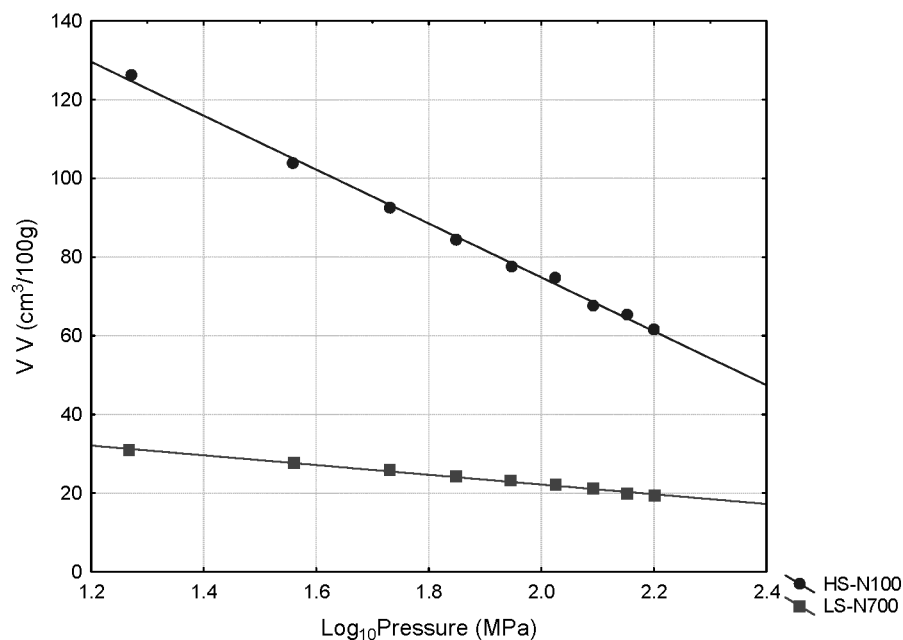


FIG. 4. — Compressed void volume and applied.

FIG. 5. — Compressed void volume versus Log₁₀ (pressure).

As observed in Figure 6, Equation 8 provides an excellent model to predict the variation of VV with pressure for any carbon black sample.

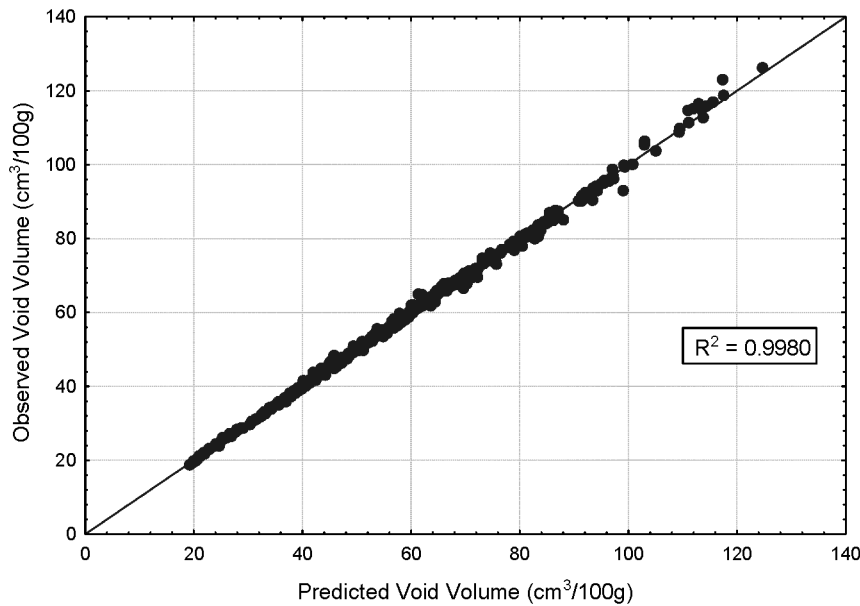


FIG. 6. — Observed and predicted void volume-log pressure model.

As previously indicated by Medalia,⁴ some deviation from the model in Equation 8 is observed for powder and heat treated samples of carbon black. This is clearly observed in Figures 7 and 8 for powder versus pelleted carbon black and for heat treated versus non-heat treated carbon black, respectively.

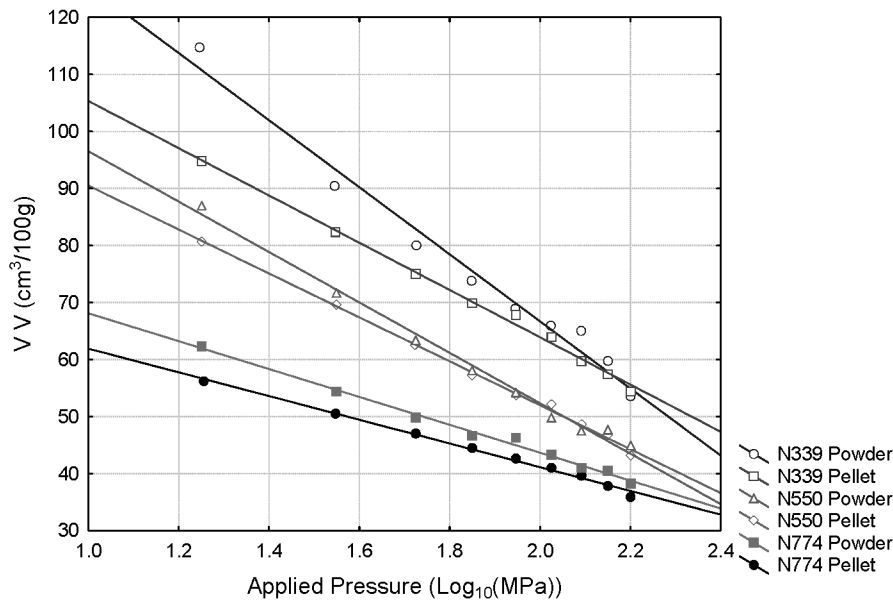


FIG. 7. — Powder and pelleted carbon black void volume.

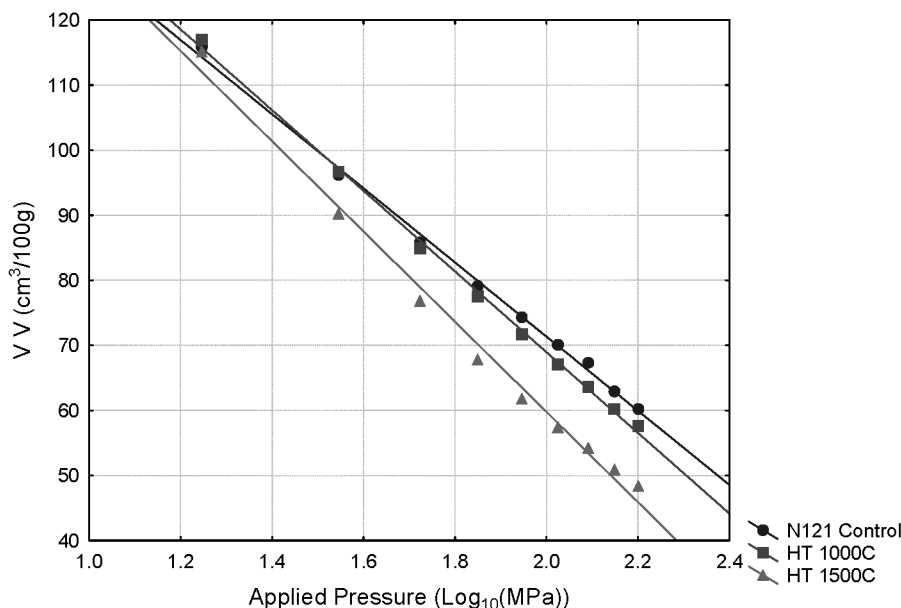


FIG. 8. — Heat treated tread carbon black compressed void volume.

The deviation observed with powder carbon blacks (average $R^2 = 0.9829$) may be the result of increased cylinder wall effect. Increased carbon black concentration at the cylinder wall may lead to a somewhat erratic, i.e. slip-stick motion, of the piston. In addition, the entrapped air in the powder samples may also lead to higher measurements of volume at a given pressure than a more air-free sample such as pelletized carbon black. This is consistent with the experimental data in Figure 7.

The plot in Figure 8 includes the data for an N121 tread carbon black and for samples of the same carbon black heat treated at 1000 °C and 1500 °C in an induction furnace as described in previous studies.⁸ All samples exhibit similar VV at low pressure, but diverge at higher pressure such that the heat treated samples exhibit decreasing VV.

Another series of heat treated carbon blacks are shown in Figure 9 for a coarser N650 type carbon black and its heat treated counterparts at 1000 °C, 1100 °C and 1500 °C. These samples were also heat treated using an induction furnace. For this series of carbon blacks the VV values are lower at any applied pressure as heat treatment temperature increases. The rate of change of VV with log P in these carcass blacks is very similar for all samples, which was not the case observed for the finer N121 series.

These results seem to indicate that heat treated carbon blacks exhibit less structure stability than non-heat treated carbon blacks, possibly due to an increase of crystallinity. In addition, large particle (coarse) heat treated carbon black grades seem to have lower structure stability at lower pressures than finer grades.

Another explanation for the behavior of the heat treated carbon blacks may be their difference in surface properties versus their non-heat treated precursors. It is well known that heat treatment of carbon black at temperatures in excess of 1000 °C leads to a significant reduction in surface functional groups (*i.e.* -OH, -COOH, etc), and ultimately to graphitization of the carbon black. A reduction of functional groups at the carbon surface may reduce the repulsive forces that arise as aggregates are brought closer together via an applied external force.

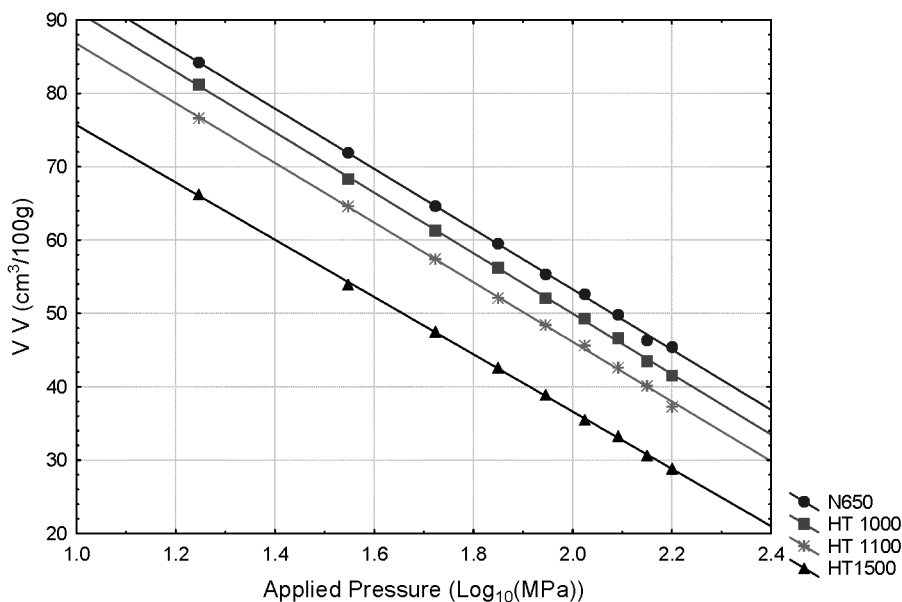


FIG. 9. — Heat treated carcass carbon black compressed void volume.

Therefore, heat treated carbon black aggregates may pack closer together than non-heat treated aggregates. The depletion of surface functional groups and/or increased crystallinity from heat treatment may lead to a reduction of secondary structure caused by loose agglomeration of carbon black aggregates. It would be expected that this effect would be more noticeable for coarser grades than for fine tread grades, which could help explain the differences between the data in Figures 8 and 9. Further work is needed to better understand the various parameters involved in VV measurements of powder and heat treated carbon blacks.

Inverse Variable Root Model. — An improved model versus the log P model for experimental data, including powder and heat treated carbon black, is described by the following equation:

$$VV = \frac{1}{A_2 + B_2 \times P^{C_2}} \quad (9)$$

Initial attempts to maintain C_2 at a constant root did not produce an improved fit versus the log model. Tables IV and V provide the regression parameters A_2 , B_2 , and C_2 for Equation 9 for all carbon blacks in this investigation. Examples of the inverse variable root model applied to three different grades of carbon black are shown in Figure 10 and demonstrate the excellent data fit for a wide level of structure and fineness. Figure 11 demonstrates the overall improvement in the goodness of fit between the inverse variable root model in Equation 9 versus the log model in Equation 8. In addition, this model provides significant improvement in the estimation of VV for powder grades.

At a given applied pressure, the inverse variable root model can be utilized for the estimation of void volume for any carbon black grade. The disadvantage with this model is the need to fit three independent parameters.

TABLE IV
INVERSE VARIABLE ROOT MODEL PARAMETERS

Sample	Grade	A ₂	B ₂	C ₂	Sample	Grade	A ₂	B ₂	C ₂
1	N762	0.01382	0.00088	0.59424	28	N650H 1000	0.00799	0.00080	0.58844
2	N660	0.01183	0.00053	0.64552	29	N650H 1100	0.00898	0.00062	0.65788
3	N650	0.00932	0.00045	0.67350	30	N650H 1500	0.01021	0.00061	0.72486
4	N220	0.00836	0.00044	0.62249	31	N774	0.01386	0.00079	0.55856
5	HV3396	0.00626	0.00041	0.63632	32	N774P	0.00859	0.00254	0.37635
6	N650	0.00898	0.00058	0.62381	33	N339P	-0.00087	0.00414	0.29358
7	N299	0.00729	0.00059	0.57906	34	N550P	0.00308	0.00281	0.38035
8	N234	0.00731	0.00047	0.60927	35	N339	0.00743	0.00064	0.55425
9	N347	0.00668	0.00066	0.57078	36	N550	0.00821	0.00083	0.56329
10	N550	0.00909	0.00046	0.66988	37	HV3396P	-0.01236	0.01343	0.14804
11	N299	0.00746	0.00059	0.57574	38	HV3396	0.00529	0.00089	0.49373
12	N330	0.00858	0.00066	0.57032	39	N135	0.00646	0.00051	0.59184
13	N762	0.01464	0.00094	0.55516	40	N134	0.00405	0.00119	0.46742
14	N774	0.01302	0.00106	0.53688	41	N330	0.00783	0.00095	0.52941
15	N121	0.00535	0.00090	0.49857	42	N220	0.00559	0.00104	0.49713
16	N121 HT1500	0.00267	0.00141	0.50241	43	N220	0.00661	0.00068	0.56758
17	N121	0.00386	0.00137	0.43719	44	N326	0.01162	0.00083	0.55271
18	N121 HT1000	0.00413	0.00105	0.50001	45	N762	0.01561	0.00075	0.62422
19	CD1006	0.02580	0.00075	0.70630	46	N762	0.01108	0.00172	0.47769
20	CD1003	0.01913	0.00230	0.44465	47	N660	0.01114	0.00044	0.70346
21	CD1001	0.00934	0.00060	0.61641	48	N660	0.01050	0.00083	0.55613
22	CD2005 HT1000	0.00059	0.00367	0.31808	49	N683	0.00664	0.00090	0.53977
23	CD2005 HT1500	0.00442	0.00089	0.60728	50	N683	0.00694	0.00076	0.56823
24	CD2005 HT2000	0.00254	0.00172	0.48347	51	N990	0.02588	0.00079	0.66739
25	CD2005	0.00362	0.00149	0.40651	52	N100	0.00411	0.00081	0.53147
26	PB-115	0.00597	0.00112	0.55088	53	N700	0.02627	0.00093	0.65227
27	N650H	0.00777	0.00081	0.56832	54	N351	0.00699	0.00074	0.55360

TABLE V
INVERSE VARIABLE ROOT COEFFICIENTS OF DETERMINATION

Sample	Grade	R ²	Sample	Grade	R ²
1	N762	0.9990	28	N650H 1000	0.9992
2	N660	0.9994	29	N650H 1100	0.9991
3	N650	0.9993	30	N650H 1500	0.9992
4	N220	0.9999	31	N774	0.9967
5	HV3396	0.9992	32	N774P	0.9921
6	N650	0.9998	33	N339P	0.9902
7	N299	0.9996	34	N550P	0.9973
8	N234	0.9997	35	N339	0.9954
9	N347	0.9993	36	N550	0.9968
10	N550	0.9992	37	HV3396P	0.9865
11	N299	0.9994	38	HV3396	0.9995
12	N330	0.9999	39	N135	0.9996
13	N762	0.9991	40	N134	0.9996
14	N774	0.9988	41	N330	0.9993
15	N121	0.9998	42	N220	0.9994
16	N121 HT1500	0.9998	43	N220	0.9995
17	N121	0.9988	44	N326	0.9988
18	N121 HT1000	0.9999	45	N762	0.9990
19	CD1006	0.9995	46	N762	0.9987
20	CD1003	0.9936	47	N660	0.9965
21	CD1001	0.9995	48	N660	0.9980
22	CD2005 HT1000	0.9976	49	N683	0.9995
23	CD2005 HT1500	0.9996	50	N683	0.9996
24	CD2005 HT2000	0.9993	51	N990	0.9984
25	CD2005	0.9995	52	N100	0.9982
26	PB-115	0.9996	53	N700	0.9972
27	N650H	0.9991	54	N351	0.9997

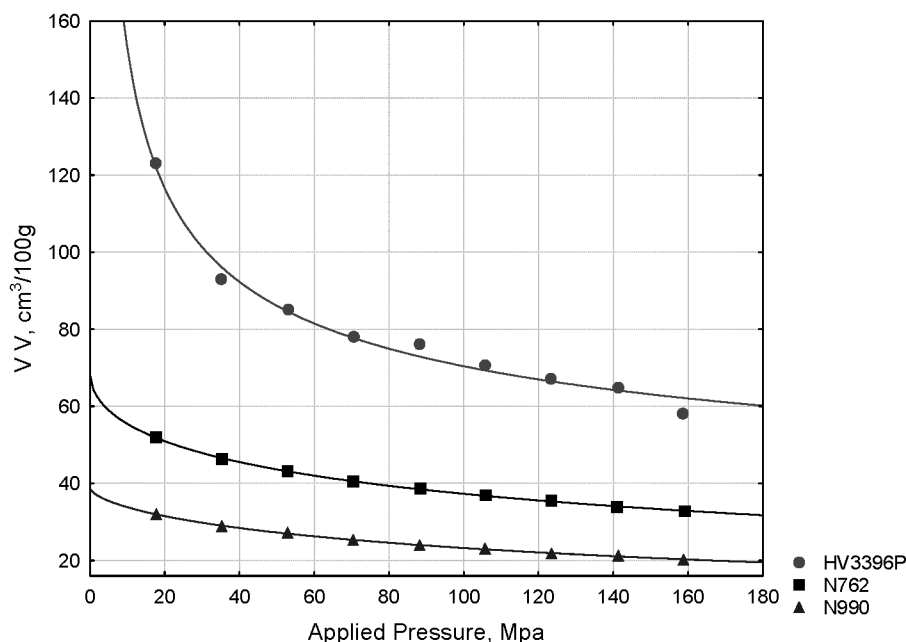


FIG. 10. — Inverse variable root model.

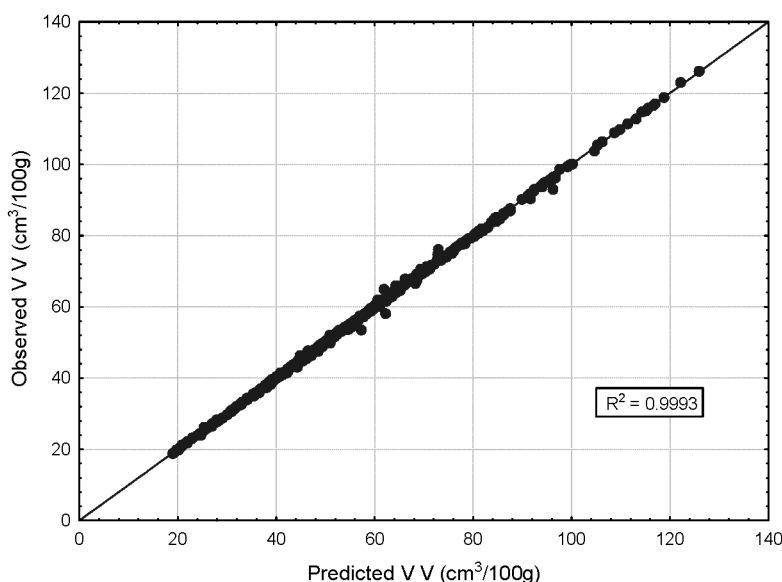


Fig. 11. — Observed and predicted compressed void volume inverse variable root model.

Work Model. — A unique feature in the experimental measurement of void volume change with pressure is the possibility of estimating the work associated with the volume change. This estimate may provide another view of the carbon black structure characterization and potentially an indication of carbon black dispersion characteristics. Under a reversible process, the work applied to bring two aggregates together should be equivalent to the work necessary to separate two aggregates to an equivalent distance. While the procedure utilized in this experiment may not be a reversible process, the work associated with the compression may indicate how easy or dif-

ficult carbon black aggregates can be separated or dispersed. The following expression can be easily derived from Equation 8:

$$P = A_3 \times e^{B_3 \times VV} \quad (10)$$

where

$$B_3 = \frac{\ln(10)}{B_1} \quad (11)$$

and

$$A_3 = e^{-\frac{A_1}{B_1} \times \ln(10)} \quad (12)$$

For the experimental set up in this investigation, the work applied by the piston to the contents of the cylinder is defined by

$$\Delta W = \int_V^{V_0} P dV \quad (13)$$

where V is the volume change in the cylinder from its initial dimension, V_0 , as pressure P is applied. In this experiment the change in volume V is the void volume VV . Therefore, P in Equation 13 can be substituted by Equation 10 so that the integral can be solved and the work calculated from:

$$W_0 = \frac{A_3}{B_3} \times e^{(B_3 \times V_0)} - \frac{A_3}{B_3} \times e^{(B_3 \times VV)} \quad (14)$$

For the cylinder in this experiment $V_0 = 846.36 \text{ cm}^3/100\text{g}$

Mathematically, A_3 and B_3 can be calculated from the log model regression coefficients A_1 and B_1 found in Table III. In order to minimize the residual errors in observed versus predicted values, A_3 and B_3 were calculated by fitting the experimental data to Equation 10 as shown in Table VI. Figure 12 presents the fitted lines for the experimental data for two types of carbon black.

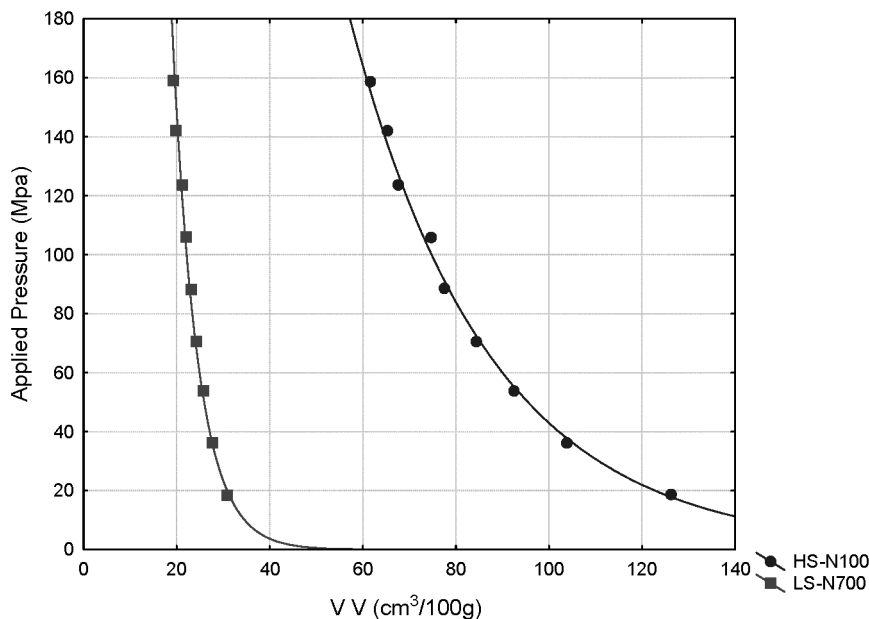


FIG. 12. — Exponential model.

Using the calculated coefficients A_3 and B_3 it is now possible to calculate W_0 from Equation 14. In this analysis, the true independent variable is P . Therefore, it is more convenient from a practical point of view to look at the variation of work, W_0 , with pressure. Solving Equation 10 for VV provides an expression similar to Equation 8:

$$VV = \frac{1}{B_3} \times \ln(P) - \frac{1}{B_3} \times \ln(A_3) \quad (15)$$

Then Equation 15 can be substituted in Equation 14, and therefore:

$$W_0 = \frac{A_3}{B_3} \times e^{V_0 \times B_3} - B_4 P \quad (16)$$

where $B_4 = -\frac{1}{B_3}$

Equation 16 indicates that the work is directly proportional to P . Figure 13 demonstrates this linearity for three different grades of carbon black. The regression values in Table VII for B_4 are indeed equal or close to equal to the reciprocal of B_3 calculated from Equation 10, as seen in Table VI. Moreover, the values of W_0 and the slope of the curves in Figure 13 align with the expected dispersion characteristics (dispersibility) of the carbon black types in this figure. Thus, CD1003 is easier to disperse than N762 and N683 with N762 easier to disperse than N683.

Further work is needed to fully validate the utility of this methodology to predict the dispersibility of carbon black in rubber compounds. However this preliminary data shows a promising result that could provide a necessary tool for the industry.

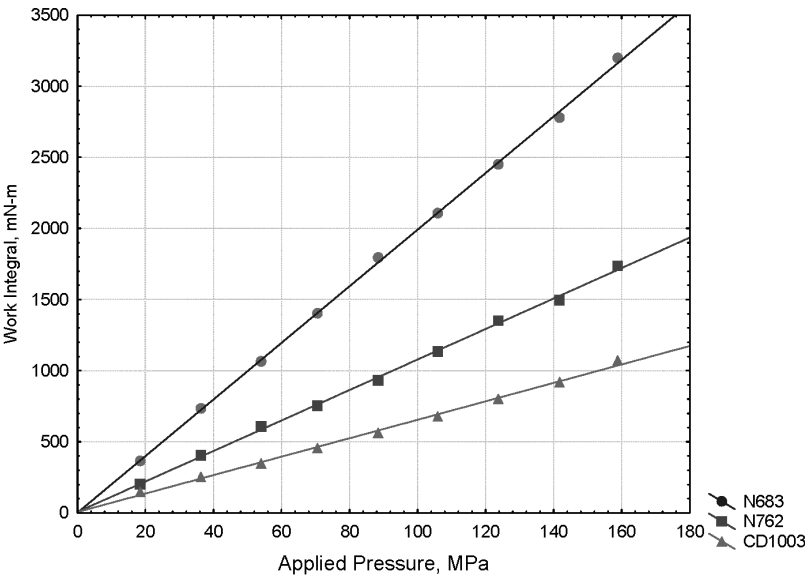


FIG. 13. — Work integral for N683, N762 and CD1003.

TABLE VI
EXPONENTIAL MODEL PARAMETERS AND COEFFICIENTS OF DETERMINATION

Sample	Grade	A ₃	B ₃	R ²	Sample	Grade	A ₃	B ₃	R ²
1	N762	2907.08	-0.093	0.9984	28	N650H 1000	1939.14	-0.056	0.9990
2	N660	2883.77	-0.075	0.9983	29	N650H 1100	1577.63	-0.055	0.9983
3	N650	1829.20	-0.056	0.9976	30	N650H 1500	1255.28	-0.055	0.9997
4	N220	3040.16	-0.055	0.9992	31	N774	862.79	-0.059	0.9893
5	HV3396	1850.38	-0.041	0.9995	32	N774P	5621.80	-0.098	0.9859
6	N650	2067.64	-0.058	0.9994	33	N339P	5171.29	-0.090	0.9707
7	N299	2490.77	-0.051	0.9995	34	N550P	1381.45	-0.039	0.9823
8	N234	2474.29	-0.048	0.9989	35	N339	2098.69	-0.058	0.9928
9	N347	2034.62	-0.048	0.9992	36	N550	2679.34	-0.051	0.9910
10	N550	1748.69	-0.055	0.9977	37	HV3396P	1930.07	-0.057	0.9762
11	N299	2692.46	-0.052	0.9988	38	HV3396	1652.22	-0.039	0.9986
12	N330	3143.46	-0.061	0.9995	39	N135	2590.44	-0.045	0.9994
13	N762	5223.48	-0.106	0.9974	40	N134	2192.53	-0.044	0.9992
14	N774	4465.40	-0.097	0.9959	41	N330	1791.58	-0.041	0.9989
15	N121	2379.01	-0.045	0.9998	42	N220	2417.68	-0.060	0.9998
16	N121 HT1500	1003.52	-0.039	0.9951	43	N220	2051.24	-0.048	0.9996
17	N121	1978.23	-0.042	0.9980	44	N326	1967.42	-0.047	0.9978
18	N121 HT1000	1532.32	-0.040	0.9990	45	N762	4369.31	-0.084	0.9971
19	CD1006	2851.45	-0.152	0.9968	46	N762	3226.98	-0.101	0.9983
20	CD1003	8245.90	-0.163	0.9826	47	N660	3297.22	-0.093	0.9985
21	CD1001	2239.46	-0.061	0.9991	48	N660	1922.04	-0.066	0.9928
22	CD2005 HT1000	1729.59	-0.043	0.9896	49	N683	3599.62	-0.076	0.9998
23	CD2005 HT1500	778.54	-0.038	0.9986	50	N683	1898.12	-0.051	0.9994
24	CD2005 HT2000	948.05	-0.041	0.9971	51	N990	1824.04	-0.050	0.9957
25	CD2005	2667.30	-0.044	0.9984	52	N100	4732.77	-0.167	0.9961
26	PB-115	1233.19	-0.050	0.9990	53	N700	1348.02	-0.035	0.9916
27	N650H	2907.08	-0.093	0.9967	54	N351	3891.65	-0.165	0.9999

TABLE VII
CUMULATIVE WORK INTEGRAL PARAMETER AND COEFFICIENT OF DETERMINATION

Sample	Grade	B ₄	R ²	Sample	Grade	B ₄	R ²
1	N762	10.669	0.9984	28	N650H 1000	18.043	0.9990
2	N660	13.189	0.9983	29	N650H 1100	18.088	0.9983
3	N650	17.632	0.9976	30	N650H 1500	16.986	0.9997
4	N220	18.044	0.9992	31	N774	9.858	0.9893
5	HV3396	24.539	0.9995	32	N774P	10.808	0.9859
6	N650	17.033	0.9994	33	N339P	24.468	0.9707
7	N299	19.659	0.9995	34	N550P	17.223	0.9823
8	N234	20.536	0.9989	35	N339	19.013	0.9928
9	N347	21.004	0.9992	36	N550	17.208	0.9910
10	N550	18.129	0.9977	37	HV3396P	24.739	0.9762
11	N299	19.070	0.9988	38	HV3396	22.199	0.9986
12	N330	16.345	0.9995	39	N135	22.701	0.9994
13	N762	9.263	0.9974	40	N134	24.518	0.9992
14	N774	10.155	0.9959	41	N330	16.693	0.9989
15	N121	22.275	0.9998	42	N220	20.975	0.9998
16	N121 HT1500	26.457	0.9951	43	N220	21.055	0.9996
17	N121	23.933	0.9980	44	N326	11.771	0.9978
18	N121 HT1000	25.516	0.9990	45	N762	9.760	0.9971
19	CD1006	6.441	0.9968	46	N762	10.702	0.9983
20	CD1003	5.912	0.9826	47	N660	15.087	0.9985
21	CD1001	16.296	0.9991	48	N660	12.948	0.9928
22	CD2005 HT1000	23.552	0.9896	49	N683	19.604	0.9998
23	CD2005 HT1500	26.341	0.9986	50	N683	19.897	0.9994
24	CD2005 HT2000	24.735	0.9971	51	N990	5.880	0.9957
25	CD2005	23.108	0.9984	52	N100	28.779	0.9961
26	PB-115	20.123	0.9990	53	N700	5.885	0.9916
27	N650H	17.887	0.9967	54	N351	19.511	0.9999

PREDICTIVE MODELING-COAN

Prior to developing product specifications for a new structure measurement based on compressed void volume, one of the most compelling uses for a void volume analyzer is to replace COAN measurements in carbon black quality laboratories. Predicting COAN data requires a good understanding of the most useful and practical void volume information, which will ultimately define the needed test parameters. Although COAN is the targeted property, OAN was also modeled in the present study and initial results suggest that the normalized OAN cannot be accurately predicted.

COAN was modeled from void volume parameters using advanced multiple and polynomial regression models. The best predictive models containing one and two predictor variables based on compressed void volume and modeled VV parameters are summarized in Table VIII.

TABLE VIII
SUMMARY OF BEST COAN PREDICTION MODELS

# Effects	n	Adjusted R ²	MS Error	Std. Error	Applied Pressure MPa	Predictor Variables
1	43	0.9564	23.36	4.83	105.9	VV
2	43	0.9600	21.96	4.69	105.9	VV, A ₂
1	36	0.9747	10.20	3.19	105.9	VV
2	36	0.9833	6.95	2.64	105.9	VV ² , C ₂

Initially forty-three carbon black samples were included in each model (all heat-treated products excluded), and adjusted R² values varied from 0.9564 for a single-term model to 0.9600 for the two-term model. The best predictor variable for a single-term model was VV at 105.9 MPa while the best two-term model included VV and the A₂ parameter from the inverse variable root model. The standard error for these models varied between 4.7 and 4.8 cm³/100g. Based on this initial assessment, we can conclude that a COAN prediction based on void volume at 105.9 MPa provided a relatively large standard error.

Analysis of the residuals indicated several non-standard carbon blacks including samples of HV-3396, CD-1003, LS-N700 and CD-1006 were responsible for the largest error. These samples represent very high surface area carbon blacks or very low surface area-low structure carbon blacks. The oil absorption characteristics of these specialty materials likely deviate from the standard grades for different reasons. High surface area blacks typically exhibit microporosity that is not observed in standard blacks, and porosity can lead to overestimated oil absorption levels. Very low structure blacks such as CD-1003 are significantly outside the calibration range of ASTM International SRB standards used to normalize OAN test data, and such a practice can lead to error. Based on these observations, the modeling was re-evaluated using only the standard grades of carbon blacks. As a result, significant improvements were observed in the best models coefficient of determination and standard error values as indicated in Table VIII. This finding would indicate that specialty blacks may require a different set of equations for COAN prediction, or that the predictive equations are a more representative measurement of structure for non-standard carbon blacks.

For the thirty-six standard grades of carbon black a single-term model using VV at 105.9 MPa has an adjusted R² value of 0.9747 with a standard error of 3.2 cm³/100g. An improved relationship is found between VV parameters and COAN using a two-term model. The best two-term model exhibits an adjusted R² value of 0.9833 at 105.9 MPa with terms including VV² and C₂. This two-term COAN prediction model has a standard error of only 2.6 cm³/100g, and appears to be an adequate model for all standard rubber grade carbon black. The following Equations 17 and 18 represent the best single and two-term COAN prediction models for standard grades, and are plotted in Figures 14 and 15.

$$COAN = -2.8150934 + 1.6809448 \times VV \quad (17)$$

$$COAN = 27.8987 + .016302 \times VV^2 + 18.9094 \times C_2 \quad (18)$$

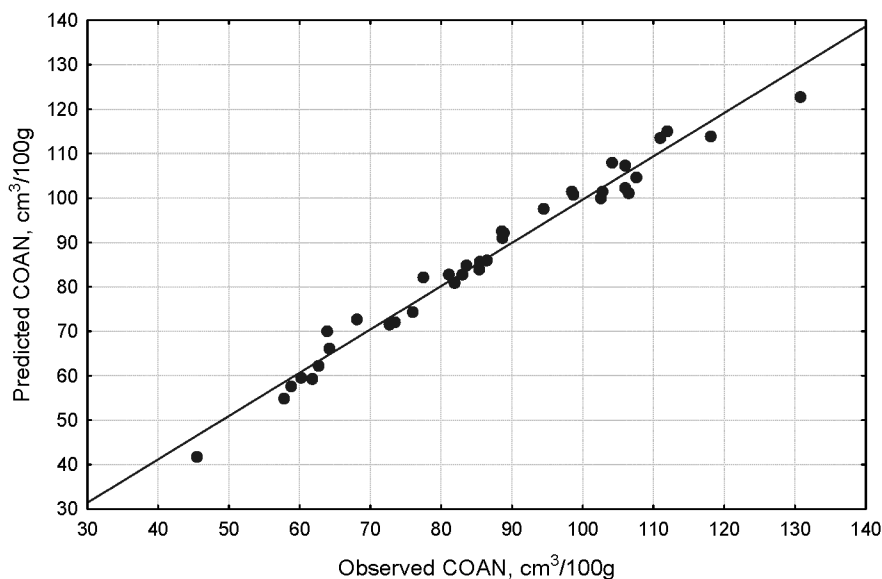


FIG. 14. — Single-term COAN prediction model for standard carbon blacks.

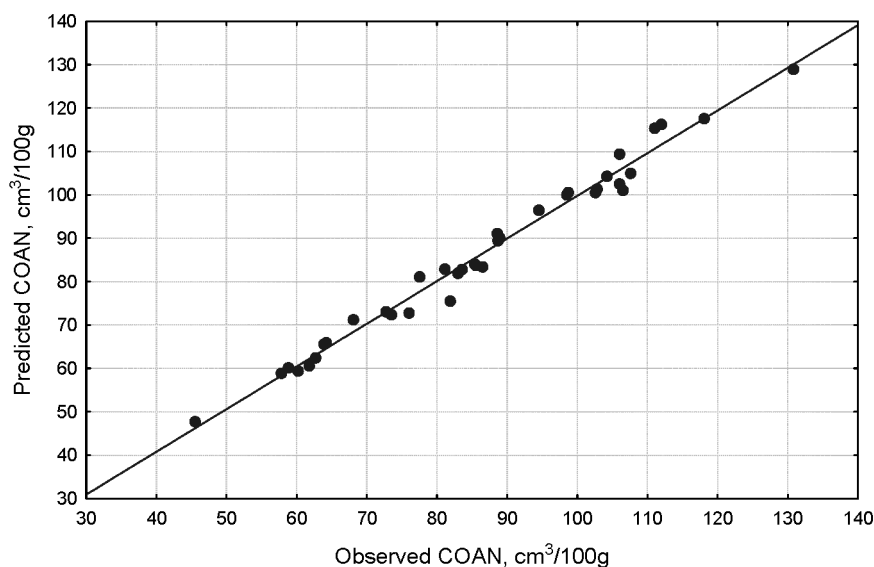


FIG. 15. — Two-term COAN prediction model for standard carbon blacks.

Based on statistical analysis of the various COAN predictor models for standard blacks, the best models utilize parameters from one or more data-fitting models. This observation indicates the void volume analysis requires multi-point testing in order to obtain model parameters. Optimization of multi-point test pressures was outside the scope of the present study.

Finally, a comparison of the best OAN and COAN single-term calculated VV models is seen in Figure 16. For this comparison, void volume data was calculated for each MPa of applied pressure using Equation 8. The coefficient of determination for the OAN model is maximized at the minimum applied pressure, while the COAN model is maximized at about 106 MPa applied pressure. The coefficient of determination for the OAN model is low, indicating a weak relationship

between compressed void volume and oil absorption numbers. Since OAN is only an estimate of carbon black structure, secondary structure and other effects related to oil-carbon black interactions result in a poor relationship with VV. Also, the normalization of OAN data may introduce bias relative to absolute VV data, possibly contributing to model error. Since OAN is currently a key structure indicator for the production of carbon black, further study of this relationship is warranted. However, the results obtained for the expression of W_0 and its potential to predict the dispersibility of carbon black may be more useful than attempting to find a correlation between VV and OAN.

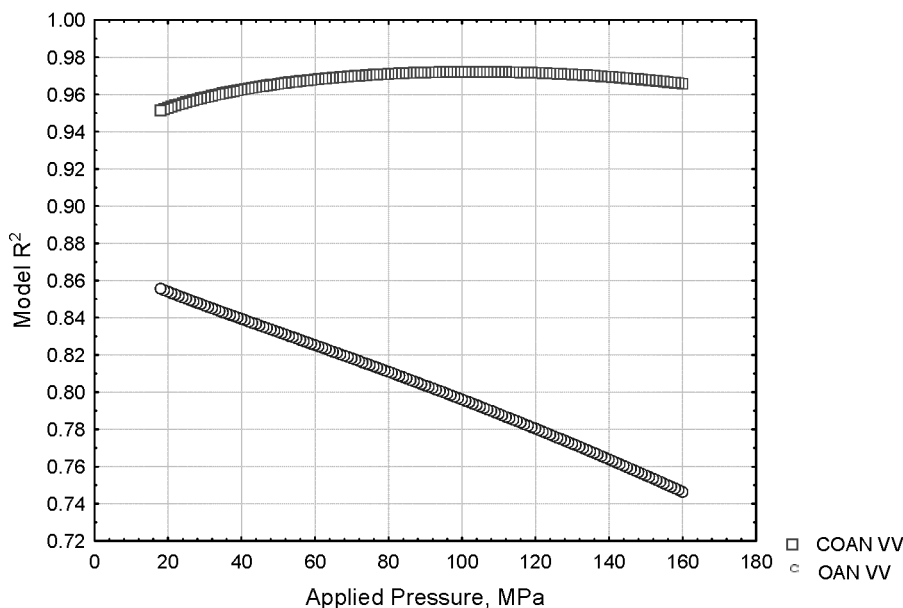


Fig. 16. — COAN and OAN prediction models based on calculated compressed void volume.

IN-RUBBER PREDICTIVE MODELING

Current carbon black structure quality testing using the mechanical oil absorptometer was accepted by the industry based on a relationship to die-swell, a processability measure of carbon black filled SBR compounds.⁹ Any new or proposed carbon black structure quality test should undergo a critical comparative analysis with existing structure methods using relevant rubber application testing that should include both processability and vulcanizate properties. This methodology insures the carbon black producer and user that a new structure measurement will not only be sensitive to variations in carbon black products, but also improve the relationships to the most prevalent applications of carbon black.

The three measures of structure including OAN, COAN and compressed void volume were modeled with RPA processability and vulcanizate properties in SBR and NR formulations using advanced multiple and polynomial regression models. Surface area measurements were also included in higher order models to observe the rubber responses to both structure and surface area.

Table IX contains the best predictive models observed for SBR compounds at constant loading using one and two predictor variables based on all three structure methods. The SBR application properties include RPA rheometer torque (Min S'), and shear modulus (G') at 1 and 10 percent SSA. Low-strain equilibrium modulus measurements were selected to maximize effects from carbon black structure while minimizing effects from carbon black particle size and surface

activity, which are more important at higher strain levels. Numerous researchers have performed studies of carbon black properties, including structure, in rubber compounds at low strain levels.¹⁰⁻¹³

TABLE IX
SUMMARY OF BEST SBR COMPOUND PREDICTION MODELS

Property	# Effects	n	Adjusted R ²	MS Error	Std. Error	Applied Pressure MPa	Predictor Variables
Min S' (ML)	2	20	0.9931	0.005210	0.0722	53	ln(NSA), W ₀
Min S' (ML)	1	20	0.9742	0.018424	0.1357	88	VV ²
G', 1%SSA	2	20	0.9897	3115.9	55.82	141	ln(NSA), W ₀
G', 1%SSA	1	20	0.9763	6775.8	82.32	88	VV ²
G', 10%SSA	1	20	0.9639	3400.6	58.31	71	VV

The best single-term models observed for minimum rheometer torque and shear modulus at 1 percent SSA contain VV² at moderate pressures. Equations for the best single-term models are as follows:

$$MinS' (ML) = -1.204652 + 0.00048065 \times VV^2 \tag{19}$$

$$G' @ 1\% = 772.427 + 0.3044 \times VV^2 \tag{20}$$

These models provide validation that compressed void volume is an improved structure measurement for rubber applications when directly compared to oil absorption methods. These single-term models for torque and shear modulus provide reasonably good coefficients of determination and standard errors as seen in Figures 17 and 18.

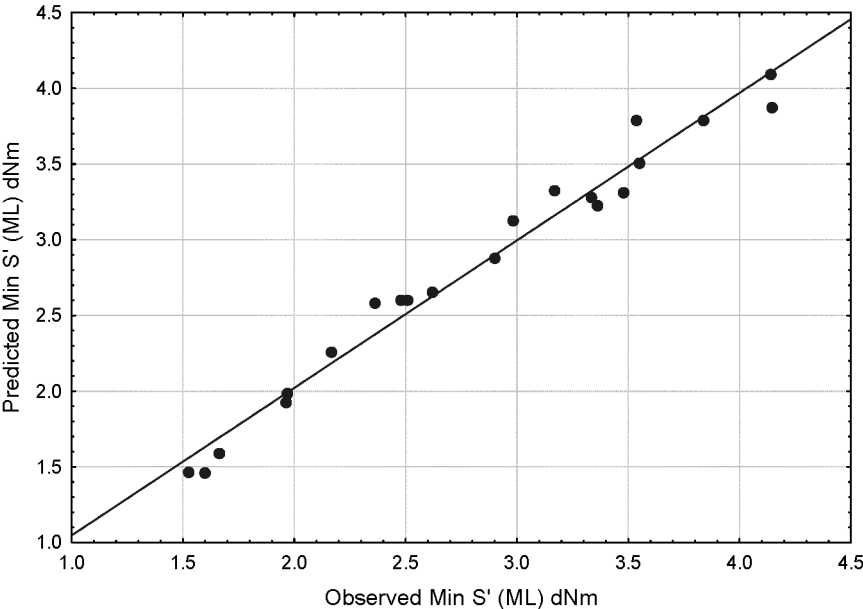


FIG. 17. — Best single-term predictive model for SBR minimum S'.

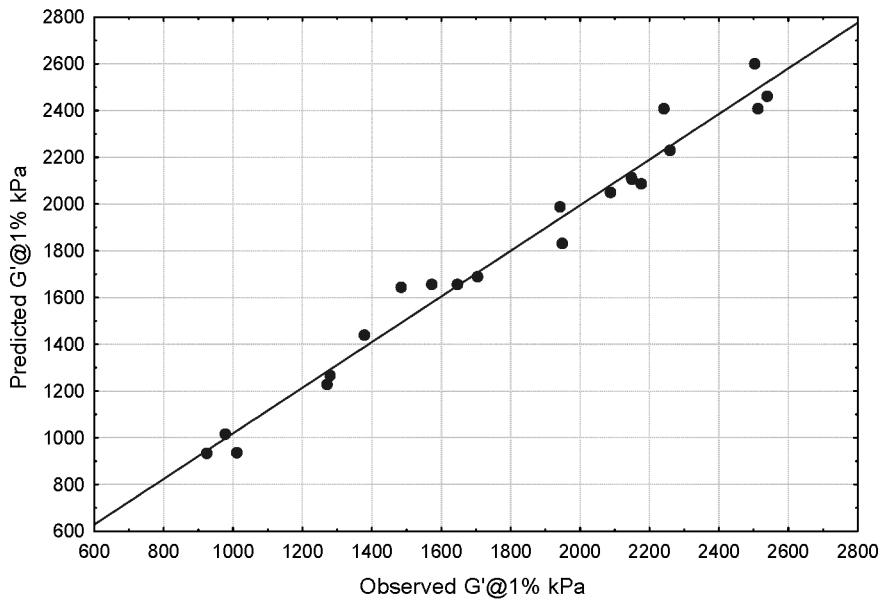


FIG. 18. — Best single-term predictive model for SBR $G'@1\%$.

A direct comparison of the single-term models R^2 for SBR rheometer torque and dynamic shear modulus at 1 percent SSA for each structure method is seen in Figures 19 and 20, respectively. For this comparison, calculated VV values from Equation 8 were generated for each MPa unit of applied pressure.

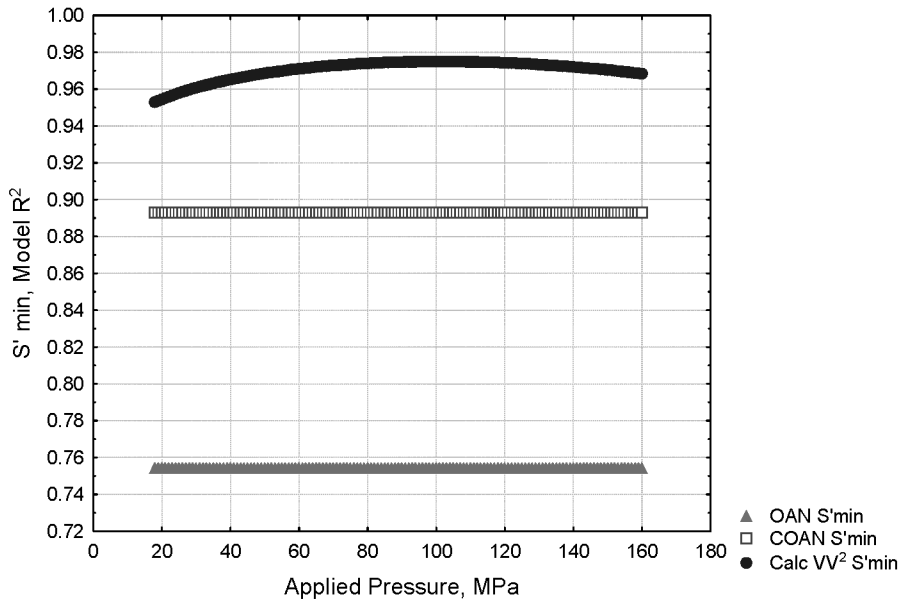


FIG. 19. — Comparison of SBR single-term model R^2 for carbon black structure tests.

These model analyses provide the most evident assessment of the relationship between structure and measurements of processability and rubber reinforcement. The compressed void volume exhibits considerable advantages over the oil absorption structure methods based on the simplest modeling, regardless of the applied pressure.

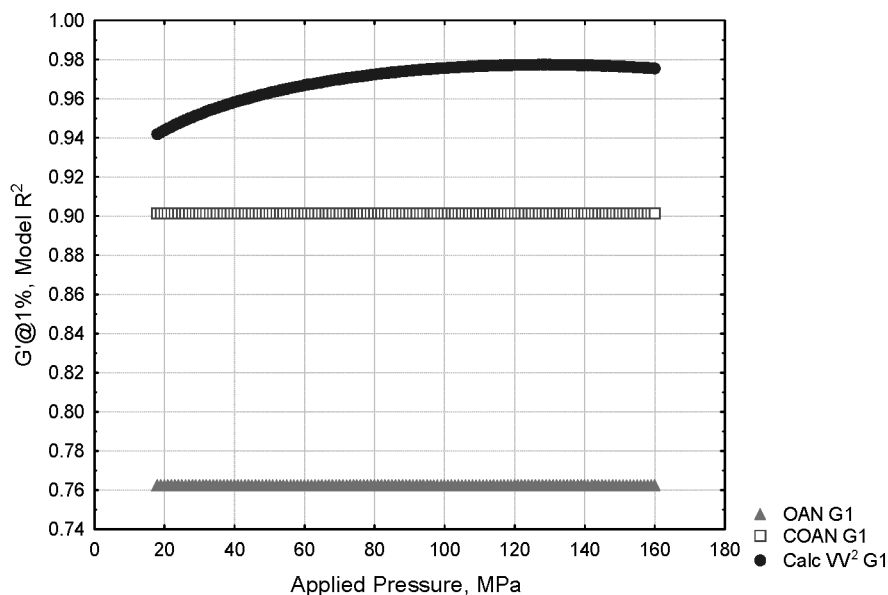


FIG. 20. — Comparison of SBR single-term model R2 for carbon black structure tests.

The best two-term models for these same rubber properties include the void volume parameter W_0 and the natural log of NSA. Ayala demonstrated that the best models of low-strain dynamic modulus of carbon black filled SBR compounds included a surface area modified effective volume fraction, V' , and this surface area measurement was the natural log of NSA.¹³ These models of surface area and structure with rheometer torque and shear modulus are displayed in Figures 21 and 22, and Equations 21 and 22.

$$S' \text{ Min}(ML) = -0.836489 + 0.641008 \times \ln(NSA) + 0.0011632 \times W_0 \quad (21)$$

$$G' @ 1\% = -511.173 + 397.8108 \times \ln(NSA) + 0.285015 \times W_0 \quad (22)$$

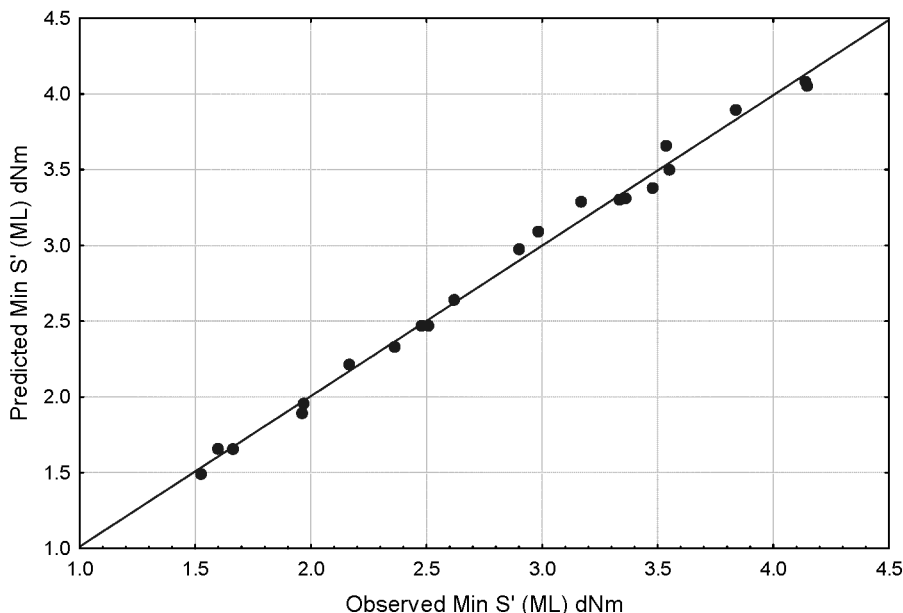


FIG. 21. — Best 2-term predictive model for SBR minimum S' (ML)

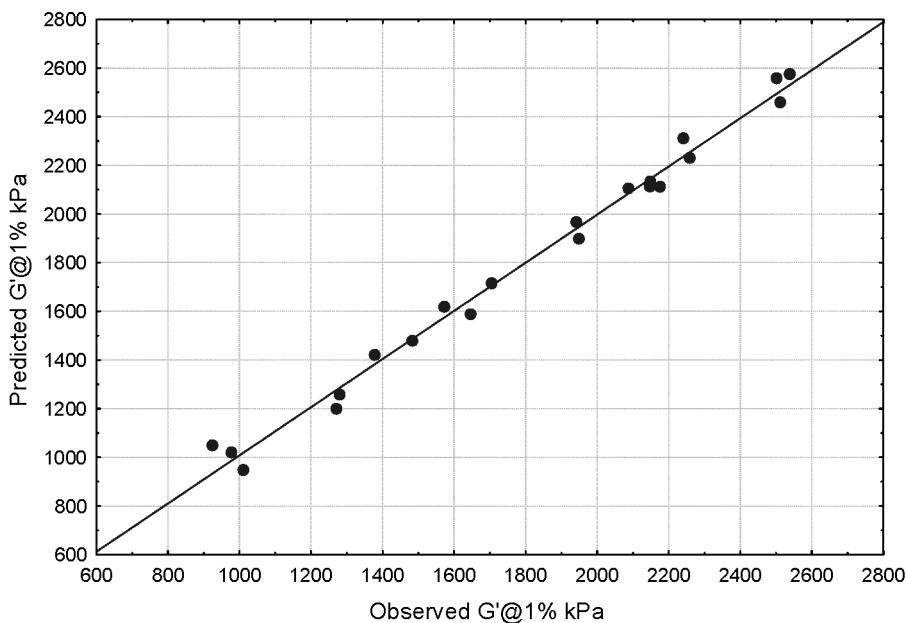


FIG. 22. — Best 2-term predictive model for SBR G' @1%.

Another interesting observation regarding the best two-term models with shear modulus at 1 and 10 percent SSA is the optimum compressive pressure for the void volume analysis. The optimum pressure interval turned out to be 141 MPa, which clearly demonstrates that the best relationship to the SBR compound is well below the compressive force of the COAN sample treatment of 165 MPa.

Modeling of natural rubber compounds (NR) was also included within the scope of this

study. The best single-term models for torque and shear modulus are seen in Figures 23 and 24. The NR compound properties exhibit slightly larger residual error than the SBR compounds as anticipated.

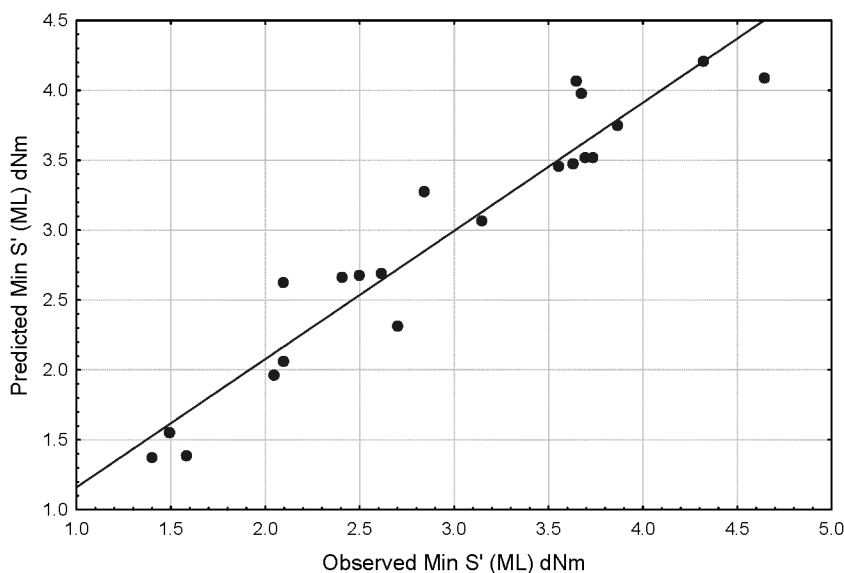


FIG. 23. — Best single-term predictive model for NR minimum S'.

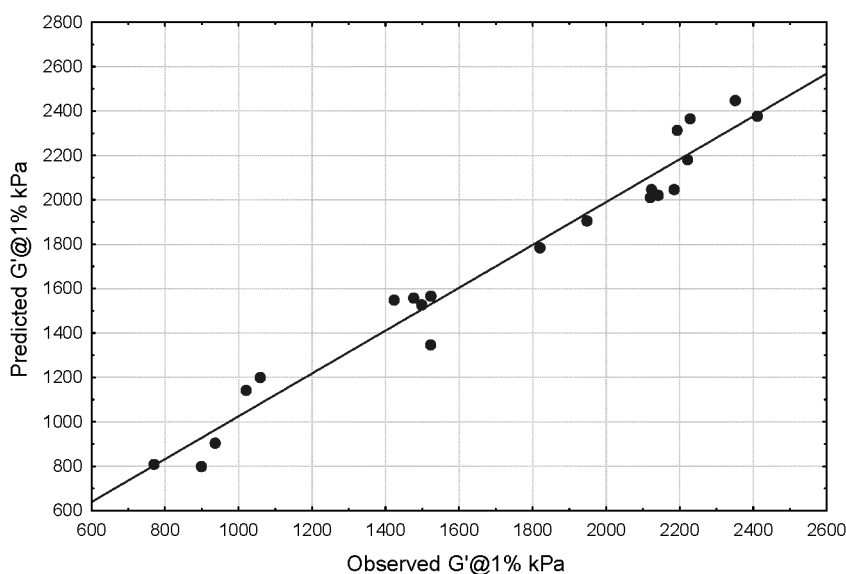


FIG. 24. — Best single-term predictive model for NR G'@1%.

The comparisons of single-term models R^2 for NR rheometer torque and dynamic shear modulus at 1 percent SSA for each structure method is shown in Figures 25 and 26, respectively. These model analyses are similar to those seen for SBR in that they provide the most evident assessment of the relationship between structure and measurements of processability and rubber reinforcement.

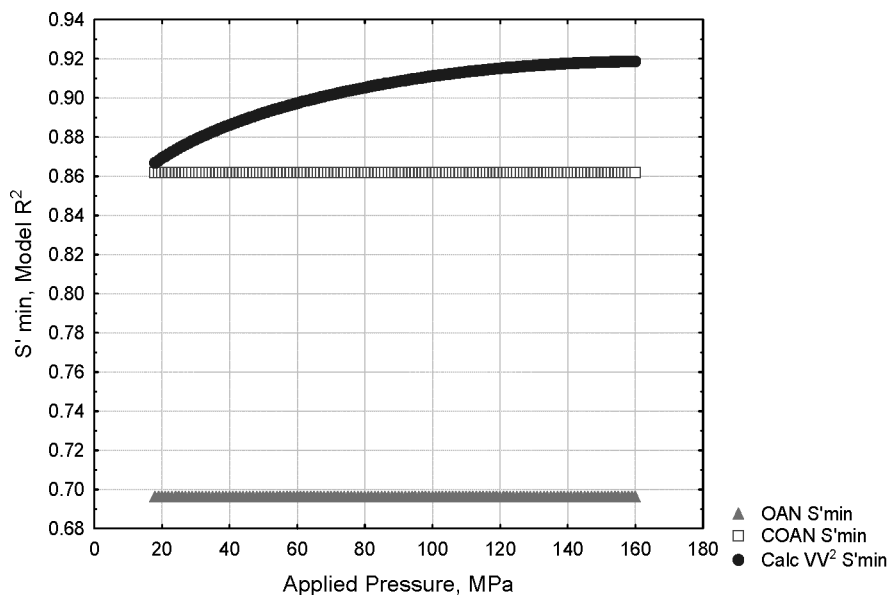


FIG. 25. — Comparison of NR single-term model R² for carbon black structure tests.

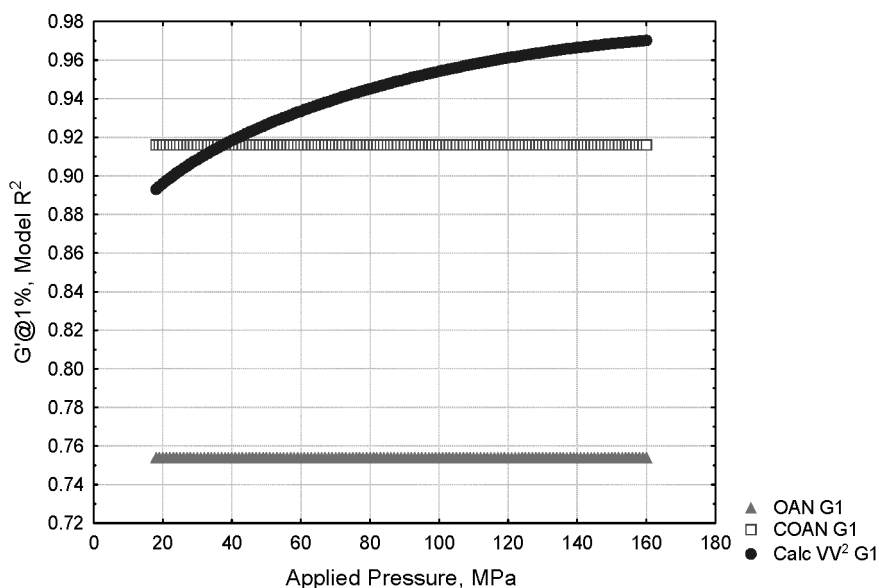


FIG. 26. — Comparison of NR single-term model R² for carbon black structure tests.

The compressed void volume provided significant advantages over the oil absorption methods based on the simplest models. The optimum NR models for both torque and shear modulus were at the maximum compressive pressure for void volume, which is an apparent indication of much greater aggregate reduction. This observation is consistent with Herd's studies of aggregate stability using TEM.¹⁴ The fact that the model R² for G' at 1 percent SSA is not yet maximized at 159 MPa, as shown in Figure 26, indicates a higher compressive force is likely needed in order to obtain the optimum carbon black VV measure for low strain shear modulus in natu-

ral rubber compounds.

Based on these modeling studies of SBR and NR compounds, the compressed void volume analysis (VV) offers a much improved measure of carbon black structure or void space which can be directly related to occluded rubber volume in rubber compounds. Optimum void volume compressive pressures varied between SRB and NR compounds. This observation provides additional evidence that a multi-point analysis of VV is needed for different applications .

SUMMARY

A detailed study of a new void volume instrument has validated equilibrium VV measurements, which indicate this rapid and simple measurement of carbon black structure is a significant improvement over oil absorption techniques. The results of this study showed that carbon black compressed void volume is more specific to primary structure of carbon black than OAN or COAN. Advancements in instrumentation and microprocessor based equipment have made it possible to commercially produce void volume instruments with sufficient accuracy, precision, and low cost that could benefit the carbon black and rubber industries.

Key observations include the following: 1) The best two-term prediction equations utilized model parameters, 2) optimal relationships between VV and compound properties varied apparently due to different levels of aggregate reduction, and 3) optimal relationships between VV and oil absorption varied at different levels of applied pressure. Therefore, VV analyzers need to be capable of multi-point analysis over a wide range of pressures.

Improvements in measurement precision should be realized through the use of digital pressure control and high accuracy pressure measurement devices. Software for new VV instrumentation would ideally incorporate the use of various model parameters for both data and predictive modeling.

Further analysis will be needed to evaluate the exponential work modeling with mixing studies to observe how well such a model can provide useful information on carbon black structure stability as it relates to dispersion and processability of rubber compounds.

ACKNOWLEDGEMENTS

The authors appreciate the significant editorial contribution by Dr. Jorge Ayala, and would also like to acknowledge Mrs. Linda Ardoin in carrying out the void volume compression testing used in this study. We also thank the Rubber Application Laboratory for providing in-rubber test measurements.

REFERENCES

- ¹ASTM International Standard Test Method D6086-05, *Ann. Book ASTM Stand.*, **09.01**, 1055 (2005).
- ²ASTM International Standard Test Method D6556-04, *Ann. Book ASTM Stand.*, **09.01**, 1075 (2005).
- ³StatSoft, Inc. (2004). STATISTICA (data analysis software system), version 7. www.statsoft.com.
- ⁴A. Medalia and R. L. Sawyer in *Proc. of the 5th Conf. on Carbon*, held at the Pennsylvania State Univ., June 19-23, 1961, New York, Macmillan, 1962, p. 563.
- ⁵A. Hoerl, "Fitting Curves to Data", *Chemical Business Handbook*, McGraw-Hill, New York (1954), sec. 20, p. 55.
- ⁶A. Medalia, *Rubber Age* **93**, 580 (1963).
- ⁷A. Voet and W. Whitten, *Rubber World* **148(5)**, 33 (1963).
- ⁸J. A. Ayala, W. M. Hess, F. D. Kistler, and G. A. Joyce, *RUBBER CHEM AND TECHNOL.* **64**, 19 (1991).
- ⁹E. R. Eaton and J. S. Middleton, *Rubber World* **152(3)**, 94 (1965).
- ¹⁰A. Medalia, *RUBBER CHEM AND TECHNOL.* **45**, 1171 (1972).
- ¹¹S. Wolf and J. Donnet, *RUBBER CHEM AND TECHNOL.* **63**, 32 (1990).

¹²E Meinecke and M. Taftaf, RUBBER CHEM AND TECHNOL. **61**, 534 (1988).

¹³J. A. Ayala, W. M. Hess, G. A. Joyce, and F. D. Kistler, RUBBER CHEM AND TECHNOL. **66**, 772 (1993).

¹⁴C. R. Herd and T. C. Gruber, "Carbon Black Aggregates: Morphology and Microdispersion in Vulcanized Rubber Compounds," paper 46 presented at ACS Rubber Division, May 5-8, 1998, Indianapolis, IN; abstract in RUBBER CHEM. TECHNOL. **71**, 831 (1998).

[Paper 101, presented at the Fall Meeting of the Rubber Division, ACS (Pittsburgh, PA)

November 1-3, 2005, revised July 2006]